HHS Public Access

Author manuscript

Am J Transplant. Author manuscript; available in PMC 2023 July 01.

Published in final edited form as:

Am J Transplant. 2022 July ; 22(7): 1766–1778. doi:10.1111/ajt.17038.

T cell depletion increases humoral response by favoring T follicular helper cells expansion

Rodrigo Benedetti Gassen[a], **Thiago J Borges**[a], **María José Pérez-Sáez**[b,c], **Hengcheng Zhang**[b], **Ayman Al Jurdi**[a], **Laura Llinàs-Mallol**[c], **Bruno Aoyama**[b], **Maurício Lima**[b], **Julio Pascual**[c], **Peter T Sage**[b], **Naoka Murakami**[b], **Leonardo V. Riella**[a,d]

[a]Center of Transplantation Science, Department of Surgery, Massachusetts General Hospital, Harvard Medical School, Boston, MA, USA.

[b]Renal Division, Brigham & Women's Hospital, Harvard Medical School, Boston, MA, USA.

[c]Department of Nephrology, Hospital del Mar, Barcelona, Spain.

[d]Department of Medicine, Division of Nephrology, Massachusetts General Hospital, Harvard Medical School, Boston, Massachusetts, MA, USA

Abstract

Antibody-mediated rejection is a major cause of long-term graft loss in kidney transplant patients. T follicular helper (Tfh) cells are crucial for assisting B cell differentiation and are required for an efficient antibody response. Anti-thymocyte globulin (ATG) is a widely used lymphocyte-depleting induction therapy. However, little is known about how ATG affects Tfh cell development and donor-specific antibody (DSA) formation. We observed an increase in circulating Tfh cells at 6 months after kidney transplant in patients who received ATG. Using an NP-OVA immunization model, we found that ATG-treated mice had a higher percentage of Tfh cells, germinal center B cells, and higher titers of antigen-specific antibodies compared to controls. ATG-treated animals had lower levels of IL-2, a known Bcl-6 repressor, but higher levels of IL-21, pSTAT3 and Bcl-6, favoring Tfh differentiation. In a mouse kidney transplant model, ATG-treated recipients showed an increase in Tfh cells, DSA and C4d staining in the allograft. Although ATG was effective in depleting T cells, it favored the expansion of Tfh cells following depletion. Concomitant use of IL-2, tacrolimus, or rapamycin with ATG was essential to control Tfh cell expansion. In summary, ATG depletion favors Tfh expansion, enhancing antibody-mediated response.

1. INTRODUCTION

Antibody-mediated rejection (ABMR) is a leading cause of long-term graft loss after kidney transplant recipients [1,2]. Although various immunosuppressive drugs have been tried as a treatment of ABMR, response rates have been poor and more effective treatments are needed [3]. For an effective humoral response, T follicular helper (Tfh) cells, a $CD4^+$ T cell subset, is critical in providing help for germinal center (GC) reactions where B cells are activated, differentiate and produce high-affinity antibodies [4]. The percentage of circulating Tfh (cTfh)

Corresponding Author: Leonardo V. Riella, MD PhD, 149 13th St, Room 5102, Charlestown, MA 02129, lriella@mgh.harvard.edu.

cells increases after kidney transplantation [5] and it is even higher in transplanted patients with pre-existent DSA [6]. These findings suggest that Tfh cells play an important role in the pathophysiology of ABMR.

Anti-thymocyte globulin (ATG) is a mix of antibodies with multiple specificities directed against lymphocytes, both T and non-T cells [7]. ATG is widely used in transplanted recipients as a lymphocyte-depleting induction therapy [8], and different mechanisms including complement activation are responsible for the T cell depletion [9,10]. Upon T cell depletion, ATG promotes a homeostatic lymphopenia-induced proliferation of memory T cells and T regulatory cells [11]. Little is known about how ATG affects the different arms of the immune response, in particular the humoral immune response, including Tfh cell development, B cell activation and differentiation.

In the present study, we analyzed circulating Tfh cells in kidney transplant recipients that had received ATG and used two murine models to better understand the effect of ATG on Tfh cells, including 1) a murine kidney transplant model, and 2) a mouse model with NP-OVA+CFA immunization, which allows tracking of antigen-specific response *in vivo*. We found that while murine ATG treatment was able to reduce total $CD4^+$ T cells in the blood and secondary lymphoid organs, it increased the percentages of antigen-specific Tfh cells and antibody-specific responses. Furthermore, we provided evidence that the low level of IL-2 and upregulation of circulating IL-21, pSTAT3 and Bcl-6 in T cells upon ATG treatment created a favorable microenvironment for the generation of Tfh cells. Combining ATG with recombinant IL-2, tacrolimus or rapamycin was essential to control Tfh cell expansion and the generation of the humoral response.

2. METHODS

2.1 Peripheral blood mononuclear cells (PBMC) isolation

We used samples from a prospective study previously published [12]. Briefly, peripheral blood samples were obtained from patients before kidney transplant and 6 months after transplant. All samples were collected at Lahey Clinic Medical Center, Burlington, MA, and processed in the Immunological Core Facility in the Transplant Research Center, Brigham and Women's Hospital. PBMCs were isolated using density-gradient centrifugation (Ficoll-Paque solution) (GE Healthcare Biosciences) and stored in liquid nitrogen.

2.2 Mice

C57bl/6 and Balb/c mice were maintained as breeding colonies in Harvard Medical School facility with water and food ad libitum. All mice used in the experiments were females between six to 10 weeks old. Animals were bred and housed in individual and standard mini-isolators under specific pathogen-free conditions. All animals were housed following the Institutional Animal Care and Use Committee (IACUC) and National Institutes of Health (NIH) Animal Care guidelines.

2.3 Murine ATG production

Murine ATG was generated as previously published [13]. Briefly, Rabbit anti-mouse thymocyte serum was generated by the Hybridoma Core at the Cleveland Clinic Research Institute by immunizing rabbits with C3H, DBA1, and SJL thymocytes. Total IgG (murine ATG) was isolated with a sequential ammonium sulfate precipitation, followed by purification with Melon gel IgG Spin Purification Kit (ThermoScientific). Total protein concentration was measured using BCA assay (ThermoScientific), and the purity was confirmed with SDS-PAGE. The efficacy of murine ATG was checked by testing $CD4^+$ and $CD8^+$ T cell depletion in the spleen, lymph nodes (LNs) and peripheral blood in naïve mice.

2.4 Immunization and treatments

C57bl/6 mice were immunized with 200 μg NP-OVA (Biosearch Technologies) emulsified in H37RA CFA subcutaneously in the flanks on day 0 and intraperitoneally treated with 500 μg of ATG or IgG control on day 0 and 4 post-immunization. At 6h, 48h and day 8 after NP-OVA+CFA immunization, blood, spleen, and lymph nodes were collected for analysis. In some experiments, mice also received treatment with 250 μg of anti-CD4 (GK1.5 clone) every two days, or daily doses of 1 mg/kg of tacrolimus/ FK-506 (Sigma), 0.5 mg/kg of rapamycin (Sigma), or 30,000 U of recombinant mouse IL-2 (Biolegend).

2.5 Kidney Transplantation model

Kidney transplantations were performed as previously described in [14,15] in a sterile environment by qualified microsurgeons. The native kidneys of the recipient remained untouched as this was a non-life-sustaining approach. Following a midline abdominal incision, the left kidney, aorta, and inferior vena cava of the donor were exposed and mobilized. The kidney was procured en-bloc including the renal vein; the renal artery, along with a small aortic cuff; and the ureter. The vessels of the graft were anastomosed end-to-side to the recipient's abdominal aorta and inferior vena cava using 10–0 nylon sutures (AROSurgical, Newport Beach, CA, United States). By using a pull-through, the ureter was directly anastomosed into the bladder. The time of cold ischemia of the graft was maintained at 40 minutes, and the warm ischemia was 30 minutes.

2.6 Flow cytometry

Spleen, blood and lymph nodes from C57bl/6 mice were collected and prepared for flow cytometry staining. Dead cells were excluded using the eBioscience Fixable Viability solution. An additional dump channel was used to exclude irrelevant cells using a mixture of antibodies (CD11c, F4/80, CD19, CD3) depending on the staining panel. Additional antibodies for CD45, CD4, PD1, CXCR5, CD25, IL-21R, CD44, B220, CD40, CD38, IgD, IgG1, Fas and GL7 were used to stain T and B cells populations. Incubation with the $OVA_{328–337}$-tetramer was performed at 37°C for 30 min before additional antibody staining. For the intracellular staining of Bcl-6, Blimp-1, T-bet, RORγT, Foxp3, and Gata-3, we used the eBioscience FOXP3 intracellular buffer following the manufacturer's instructions. All antibodies used were from Biolegend.

For pSTAT detection, cells were fixed with 1% PFA in PBS for 10 min at room temperature, permeabilized with True-Phos Perm Buffer (BioLegend) at −20°C, and stained with mouse anti-Stat5 (pY694, BD) and anti-Stat3 (pS727; BD) alongside surface-stain antibodies detailed above in permeabilization buffer (eBioscience). Samples were acquired using an LSRFortessa (BD) and analyzed using FlowJo (BD).

3.6 Flow cytometry sorting and in vitro cocultures

After 7 days of NP-OVA+CFA immunization, spleen and draining lymph nodes from ATG or IgG-treated mice were harvested and cells were incubated with Fc Block and fluorochrome-conjugated anti-CD3, anti-CD4, anti-CD19, anti-ICOS and anti-CXCR5 for 30 min on ice. First, CD4 T cells ($CD3^+CD4^+CD19^-$) and B cells ($CD3^-CD4^-CD19^+$) were sorted and co-culture *in vitro* in different combinations in an incubator at 37°C with 5% of CO_2. As a positive control, we used 2μL/mL of anti-CD3 and 5μL/mL of anti-IgM antibodies. After 6 days of incubation, the supernatant was stored for antibody quantification and cells were stained with anti-CD19, anti-MHCII and anti-GL7 and analyzed with a flow cytometer. In some experiments, cells were sorted further as Tfh ($CD3^+CD4^+CXCR5^+ICOS^+CD19^-$) and non-Tfh ($CD3^+CD4^+CXCR5^-ICOS^-CD19^-$) cells.

2.8 ELISA for NP, OVA-specific antibody, IL-2, IL-21, and Donor Specific Antibody Measurement

For NP or OVA-specific antibody ELISAs, Maxisorp plates were coated with 1μg/mL of NP-BSA (Biosearch Technologies) or OVA (InvivoGen), followed by blocking for 1 hour with BSA (5% BSA, 0.05% tween in PBS 1X buffer) and mice serum was added in a dilution of 1/5000 and incubated for 2 hours at room temperature. Rabbit anti-mouse antibody HRP-conjugated (Invitrogen) and TMB (Life Technologies) were used for development. IL-2 and IL-21 concentrations in serum were determined by capturing ELISA (R&D Systems), according to the manufacturer's instructions. Plates were read on a plate reader (Spectramax).

For the donor specific-antibody measurement, we used Balb/c or C57bl/6 mice as probes for DSA quantification in the serum. 5×10^5 splenocytes were added to 96-well plates and after two washes, the cells were incubated for 30 minutes with serum from naïve, POD7, POD14 and POD20 of IgG-treated mice or ATG-treaded mice (1:40 dilution). Cells were then stained with Fixable viability Dye (eBioscience), anti-B220 (Biolegend) and anti-CD3 (Biolegend) in the presence of Fc-block (Biolegend). Cells were washed twice and incubated for 30 minutes with anti-IgG and anti-IgM (BDbioscience). Donor reactive antibody against MHC class II was measured by assessing anti-IgG or anti-IgM signal on total $B220^+$ cells and against MHC class I by assessing anti-IgG or anti-IgM signal on total $CD3^+$ cells by flow cytometry and expressed as mean fluorescence intensity (MFI).

2.9 H&E and C4d staining

For H&E staining, kidneys were fixed with 10% formalin, embedded in paraffin and cut into 5 μm sections. Hematoxylin and eosin staining were performed by standard methods [16] to evaluate the cell infiltration.

Deposition of C4d in the kidney tissue was stained using a rat anti-mouse C4d antibody with a FITC-conjugated anti-rat secondary antibody. Briefly, frozen sections (8 μm) fixed with acetone were washed with PBS three times. The sections were blocked with PBS containing 1% bovine serum albumin (BSA) at room temperature for 1 hour. The sections were stained by rat anti-mouse C4d antibody (clone 16D2, Novus Biologicals) diluted 1:100 with PBS containing 1% BSA, followed by FITC-conjugated anti-rat IgG antibody (Jackson ImmunoResearch) diluted 1:1000 for 1 hour at room temperature. After washing 3 times with PBS, the fluorescent images were captured with a fluorescence microscope (Zeiss LSM 780).

Statistical analysis

Data were tested for normality of distribution using a Kolmogorov-Smirnoff test. Differences between groups were analyzed with unpaired t-tests for two groups or a one-way ANOVA test for >2 groups followed by a Tukey correction for multiple pairwise comparisons. GraphPad Prism software (San Diego, CA, USA) was used for statistical analysis. All tests were two-sided and an α level of 0.05 was considered significant. Values shown in graphs represent the mean ± standard deviation (SD).

3. RESULTS

3.1 Circulating Tfh cell percentages increase after kidney transplant in ATG-treated patients

To assess the kinetics of cTfh in kidney transplant patients who received induction therapy with ATG, we collected and analyzed PBMCs of these patients before and after transplantation (Fig. 1A). Briefly, this cohort was composed of kidney recipients with a mean age of 59 years old that received 3 doses (0.75 mg/Kg per dose) of rabbit ATG, 30% of the cohort were females and the leading cause of kidney disease was diabetes. In addition, deceased donors represented 70% of the cohort while all patients were non-sensitized (PRA of zero) [12]. The demographics of the cohort are detailed in Supplementary Table 1. Overall, we found an increase in cTfh cell ($CD4^+CXCR5^+PD\text{-}1^+$) percentages six months after transplantation compared with pre-transplantation (Fig. 1B–C), although total $CD4^+$ T cells remained significantly depleted (Fig. 1D).

3.2 Increase in DSA and C4d staining generated by ATG in a kidney transplant model

We further assessed the capacity of ATG to modulate Tfh cells and alloantibody response in a non-survival-based model of kidney transplantation. BALB/c kidneys were transplanted into C57Bl/6 mice and the recipients were treated with ATG (murine) or IgG control at post-operatory day (POD)0 and POD4 (Fig. 1E). The flow cytometry gating strategy for Tfh and B cells can be seen in Supplementary Figure 1. ATG treatment successfully decreased the percentages of $CD4^+$ T cells in the blood (Supplementary Figure 2A). However, the percentage of cTfh cells were higher in the blood of ATG-treated mice at POD7 and POD20 compared to controls (Fig. 1F), while no differences were seen in the absolute number of Tfh, total B cells and GC B cells in the spleen at POD20 (Fig. 1G–I). Nonetheless, the percentage and the absolute number of $IgG1^+$ B cells in the spleen (Fig. 1J) and the serum levels of anti-MHC class I and class II DSAs (Fig. 1K) were higher in the animals treated

with ATG compared to IgG controls. To evaluate whether higher levels of DSAs were associated with greater alloantibody-mediated injury, we analyzed the kidney allografts for immune infiltration by H&E and antibody-allograft interaction with complement activation by C4d staining. We found tubulitis and interstitial inflammation in both ATG and IgG-treated mice but more significant microvascular inflammation (glomerulitis and peritubular capillaritis) in ATG-treated mice compared to controls (Fig. 1L). We also found stronger C4d staining in peritubular capillaries in ATG-treated mice compared to IgG-treated mice (Fig. 1M). Taken together, these data indicate that ATG treatment alone is associated with increased generation of an early alloantibody response and antibody-mediated allograft injury in a kidney transplantation model.

3.3 Antigen-specific Tfh cells were enriched in LNs after ATG treatment

To better understand the impact of ATG on Tfh cells, we used a murine model of NP-OVA immunization and analyzed whether ATG could modulate the formation of Tfh cells. C57Bl/6 mice were immunized with NP-OVA + CFA at day 0 and treated with murine ATG or IgG control at days 0 and 4. On day 8 after immunization, cells from peripheral blood and secondary lymphoid organs were analyzed (Fig. 2A). ATG-treated animals had lower percentage and absolute numbers of $CD4^+$ T cells in the draining lymph nodes (Fig. 2B–C), blood and spleen (Supplementary Figure 2B). When we analyzed the Tfh cell ($CD4^+CXCR5^+PD\text{-}1^+$) compartment, the percentages and absolute numbers were increased in the ATG-treated group compared with the IgG control group (Fig. 2D–E). In addition, the proportion of OVA-specific $CD4^+$ Tfh cells was higher in ATG-treated animals, but ATG treatment did not affect the percentage of OVA-specific non-Tfh cells compared to IgG treatment (Fig. 2F).

3.4 ATG increased antigen-specific humoral response

Based on the expansion of Tfh cells, we next tested the effect of ATG on GC formation and antigen-specific antibody production after NP-OVA immunization. On day 8 after immunization, the percentage of total B cells (Fig 3A–B), GC B cells (Fig 3C–D) and class-switched $IgG1^+$ B cells (Fig 3E–F) in the draining lymph nodes were higher in the ATG-treated group compared to IgG-treated control group. In blood and spleen, the action of ATG was similar to the lymph nodes (data not shown).

To prove that the increase of Tfh and B cells by ATG might induce specific antibody production, and this activation was dependent on $CD4^+$ T cells, we depleted $CD4^+$ T cells using a murine anti-CD4 monoclonal antibody in our model of NP-OVA immunization and analyzed the amount of specific IgG in serum by ELISA. On day 8, NP-specific (Fig 3G) and OVA-specific (Fig 3H) serum IgG were increased in ATG-treated mice. However, no detectable IgG was found in the absence of $CD4^+$ T cells. These results highlight the capacity of ATG to induce an antigen-specific humoral response in a $CD4^+$ T cell-dependent manner.

3.5 Total CD4+ T cells from ATG-treated mice have greater capacity in enhancing B cell response

To determine the capacity of $CD4^+$ T cells from ATG-treated mice to increase humoral immune responses we used an *in vitro* CD4-mediated B cell stimulation assay [15,17]. Briefly, animals were immunized with NP-OVA+ CFA with or without ATG treatment, and after 8 days, total B cells (gated as $CD3^-$ $CD19^+$), $CD4^+$ T cells (gated as $CD3^+CD4^+CD19^-$) or Tfh cells (gated as $CD3^+CD4^+ICOS^+CXCR5^+$ $CD19^-$) were sorted from the spleen of ATG- or IgG-treated mice. Cells were cocultured for 6 days with anti-CD3 and IgM stimulations. B cells in the presence of either $CD4^+$ T cells from ATG or IgG-treated mice increased the frequency of $IgG1^+GL7^+$ GC B cells. However, we saw enhanced B cell differentiation to class-switched B cells when B cells were cocultured in the presence of $CD4^+$ T cells from ATG-treated mice (Fig. 4A–B). Similarly, there was greater evidence of IgG1generation in the co-cultures with ATG-treated $CD4^+$ T cells (Fig. 4C). In contrast, the B cell helper capacity in the presence of Tfh cells from ATG or IgG-treated mice showed no difference (Fig. 4D–F). Together, these data demonstrate that ATG expanded the proportion of Tfh cells in the pool of total $CD4^+$ T cells but did not increase the helper capacity of Tfh cells on a per-cell basis.

3.6 Tacrolimus or rapamycin combination with ATG blocked the humoral response induced by ATG

Based on the low incidence of early antibody-mediated rejection post-transplant in ATG-treated kidney patients, we hypothesized that additional immunosuppression agents may contribute to mitigating Tfh cell expansion and B cell activation upon ATG treatment. To test this, we used the same NP-OVA model as depicted in Fig. 1D, but mice were now treated with ATG in combination with either tacrolimus or rapamycin. Serum and lymph nodes were analyzed at day 8 post-immunization (Fig. 5A). We found that the ATG in combination with tacrolimus or rapamycin was able to decrease the total $CD4^+$ T cells percentages and absolute numbers compared with the group treated only with ATG (data not shown). Moreover, both combinations successfully decreased the absolute numbers of Tfh cells (Fig. 5B–C), GC B (Fig.5 D–E), $IgG1^+$ B cells (Fig. 5F–G) and NP- and OVA-specific antibodies (Fig. 5H–I). Therefore, ATG must be combined with other immunosuppressive drugs to prevent Tfh cell expansion and the generation of the humoral response.

3.7 IL-2 deficiency upon T cell depletion with ATG drives Tfh differentiation

To investigate the capacity of ATG to induce Tfh cell expansion, we evaluate the signals needed to induce the differentiation of Tfh cells. We first evaluate the capacity of ATG to induce the differentiation of other $CD4^+$ T cells subsets besides Tfh cells. ATG-treated mice also had an increase in the proportion of regulatory T cells while no significant changes were observed in Th1, Th2, or Th7 phenotypes compared with control mice (Fig. 6A). In addition, ATG increased serum levels of IL-21 at 48 hours after immunization with NP-OVA (Fig. 6B). On the other hand, the Bcl-6 repressor cytokine IL-2 was decreased in the serum 6 hours after immunization with NP-OVA in ATG-treated mice (Fig. 6C). This suggests that less IL-2 availability caused by ATG induced T-cell depletion creates a favorable environment for Tfh differentiation (Fig. 6D). To test this hypothesis, we restore IL-2 levels

in NP-OVA immunized and ATG-treated mice by treating the animals with i.p. injections of 30000 U of recombinant murine IL-2 twice a day for 8 days (Fig. 6E). ATG treatment was associated with an increase in the expression of pSTAT3 (Fig. 6F) and the transcription factor Bcl-6 (Fig. 6G) on $CD4^+$ T cells from draining lymph nodes. The restoration of IL-2 in ATG-treated mice decrease Bcl-6 (Fig. 6G) expression but not pSTAT3 (Fig. 6F) on $CD4^+$ T cells. In contrast with ATG-treated animals, ATG + IL-2 treatments induced pSTAT5 (Fig. 6H) and Blimp-1 (Fig. 6I) upregulation on $CD4^+$ T cells in draining lymph nodes. The combination of ATG + IL-2 was also able to control the enhancement of Tfh cells (Fig. 6J), GC B cells (Fig. 6L), $IgG1^+$B cells (Fig. 6M) and NP-specific antibody production (Fig. 6N). Taken together, the low levels of IL-2 induced by ATG treatment were able to activate pathways responsible to promoted Tfh cells differentiation and antibody production. The restoration of IL-2 in the microenvironment block ATG-induced humoral response.

4. DISCUSSION

Antibody-mediated rejection is a major cause of graft loss and T follicular cells play an essential role in the generation of an antigen-specific antibody response. In the present study, we demonstrated that antithymoglobulin (ATG) induction leads to an expansion of Tfh cells and enhances humoral response in the absence of additional immunosuppressive drugs. We used two *in vivo* models (NP-OVA immunization and a kidney transplant model) to assess Tfh cells, B cell maturation and antigen-specific antibody generation. Furthermore, we identified that T-depletion by ATG created a favorable environment for Tfh cell expansion with low IL-2 levels and high IL-21. Thus, our data demonstrate that ATG treatment favors antigen-specific Tfh expansion, enhancing antibody-mediated response.

Rabbit ATG is used as induction therapy in over 70% of all kidney transplants performed in the USA [18]. It is the most common T-cell depletion agent used in the clinic, though some transplant centers use alemtuzumab, an anti-CD52 monoclonal antibody, as an alternative. ATG induces a fast and sustained T cell depletion in the circulation and secondary lymphoid tissues by targeting a combination of T cell antigens, inducing complement-mediated cell death. Under lymphopenic conditions, remaining T cells undergo substantial homeostatic expansion[19]. The expanding lymphocytes have a dominant memory phenotype and this homeostatic proliferation has been proposed as a major barrier to the induction of transplant tolerance [20,21]. Our study further contributes to this finding by indicating that during homeostatic proliferation, T follicular helper cells are preferentially expanded, with the potential to promote humoral response. Indeed, the severe T-cell depletion by alemtuzumab has been associated with a higher risk of antibody-mediated rejection in particular when drug minimization was attempted post-transplant [22,23]. Clinical trials comparing rabbit ATG and non-depleting induction therapies showed the benefit of ATG induction in sensitized patients [24,25]. Therefore, we think that concurrent adequate maintenance immunosuppression in the early post-transplant period is key to arresting this Tfh expansion irrespective of lymphocyte count. Furthermore, withdrawing CNI at 6 months post-transplant in low immunological risk patients that received ATG induction may also be associated with de novo DSA generation in up to 42% of patients as it has been shown by Hricik et al. in the CTOT-9 trial [26]. Delaying initiation, dose minimization or withdrawal

of calcineurin inhibitors may favor the development of an antibody-mediated alloimmune response.

High-affinity antibodies result from the contact between Tfh cells and B cells in germinal centers, and this interaction has recently been implicated as fundamental to modulate antibody-mediated rejection [27]. We observed an increase in the percentages of cTfh cells at 6 months after transplant in kidney transplant patients that received ATG as an induction even though maintenance therapy was started at post operatory day 1. Similar to our findings, Tfh cell activation in ATG-treated patients was also found by Macedo et al. In their study, they compared 31 kidney transplant patients that received ATG with 20 kidney transplant patients that received basiliximab for induction therapy [28]. ATG treated-patients showed upregulation of PD-1, and an activated and highly proliferative profile of Th1-like cTfh cells. Moreover, the percentage of effector memory cTfh cells and serum IL-21 in DSA^+ patients was significantly higher than those of stable patients in the ATG group [28]. In face of the deleterious effect of the DSA in kidney allograft survival [29 30], it is crucial to control the expansion of Tfh cells with the right dose and timing of other immunosuppressive drugs such as tacrolimus to prevent DSA formation.

We propose that ATG modify the immune environment by favoring the pathways responsible for inducing Tfh cell development. The phosphorylation of STAT3, the transcriptor factor Bcl6, and the cytokine IL-21 have broad effects on Tfh cell biology and provide insight into how regulation of these signals mediates naïve $CD4^+$ T cells differentiation into Tfh cells [31–33]. Bcl6 and pSTAT3 expression were increased in ATG-treated mice, and this was reflected in the amount of IL-21 in the serum. Higher IL-21 levels in the serum using a T cell-depleting agent (alemtuzumab) was also observed by Jones et al [34]. Although the authors did not focus in the antibody response, they showed secondary autoimmunity following alemtuzumab treatment of multiple sclerosis patients and higher T cells apoptosis driven by an increase in IL-21 [34].

Another important factor that interferes with Tfh differentiation is the cytokine IL-2. IL-2 is known to induce the expression of the transcription factor Blimp-1, responsible for controlling the terminal differentiation of B cells into antibody-secreting plasma cells. However, Blimp1 represses the expression of Bcl6 [35]. The balance between Blimp-1 and Bcl6 expression is thought to control the relative commitment of $CD4^+$ T cells into the Tfh pathways [36,37]. In addition to Blimp-1, the phosphorylation of STAT5, which is potently activated by IL-2, antagonizes this process preventing Tfh cell differentiation and favoring the differentiation of other $CD4^+$ T cell subsets [38]. Since the primary source of IL-2 comes from T cells [39], we observed depletion in IL-2 when we evaluated its levels in the serum after NP-OVA immunization and the first dose of ATG. Along those lines, recombinant IL-2 was demonstrated to inhibit Tfh responses and antibody production against influenza in the absence of T regulatory cells [38]. Moreover, low doses of IL-2 are also known to induce T regulatory cells in mouse models and can be used as a treatment to control graft rejection [40] and autoimmune diseases [41]. In our model, in addition to Tfh cells enrichment, we observed an expansion of the T regulatory phenotype but no increase in T follicular regulatory cells (Supplementary Figure 2C). These data align with studies that indicated that $CD4^+$ T cells subsets might have different ATG-susceptibilities [42]. Lastly, we found that restoring IL-2

levels in ATG-treated mice blocked the signals required in Tfh differentiation by inducing pSTAT5 and Blimp-1.

In conclusion, we are not questioning the benefits of T cell depletion by ATG as it has clearly been shown as effective induction therapy in high-risk patients when used in combination with other immunosuppressive drugs for the prevention of acute rejection [43]. However, understanding the mechanisms of action of immunosuppressive drugs is essential to find the best combinations and timing to maximize the suppression of effector T cells, reduce the risk of infection, side effects and alloantibody responses. Furthermore, measuring circulating Tfh cell numbers, IL-2 and IL-21 in addition to the current standard of measuring circulating anti-HLA antibodies in the serum could be a potential marker of patients at higher risk of antibody-mediated rejection. Based on our data, delaying CNI initiation after ATG induction in patients with delayed graft function may lead to deleterious effects by favoring the development of Tfh cells and potentially promoting alloantibody generation.

Supplementary Material

Refer to Web version on PubMed Central for supplementary material.

Acknowledgments

This work was in part supported by the following research grants: National Institute of Health (NIH) Grant R01 AI143887 (to L.V.R.), the Assistant Secretary of Defense and Health Affairs, through the Reconstructive Transplant Research (RTR), under Award No. W81XWH2010758 and W81XWH2110904 (to L.V.R.). Opinions, interpretations, conclusions, and recommendations are those of the author and are not necessarily endorsed by the Department of Defense; T.J.B. is a recipient of a post-doctoral fellowship grant from the American Heart Association (AHA). This study was in part supported by the Harold and Ellen Danser Endowed Chair in Transplantation at Massachusetts General Hospital (Boston, MA, USA). Cartoons were created with BioRender.com.

REFERENCES

1. Halloran PF et al. Disappearance of T cell-mediated rejection despite continued antibody-mediated rejection in late kidney transplant recipients. J. Am. Soc. Nephrol 26, 1711–1720 (2015). [PubMed: 25377077]
2. Sellarés J et al. Understanding the causes of kidney transplant failure: The dominant role of antibody-mediated rejection and nonadherence. Am. J. Transplant 12, 388–399 (2012). [PubMed: 22081892]
3. Böhmig GA, Eskandary F, Doberer K & Halloran PF The therapeutic challenge of late antibody-mediated kidney allograft rejection. Transpl. Int 32, 775–788 (2019). [PubMed: 30955215]
4. Sage PT & Sharpe AH T Follicular Regulatory Cells in the Regulation of B cell Responses. Trends Immunol. 1–9 (2015) doi:10.1016/j.it.2015.05.005.
5. Cano-Romero FL et al. Longitudinal profile of circulating T follicular helper lymphocytes parallels anti-HLA sensitization in renal transplant recipients. Am. J. Transplant 19, 89–97 (2019). [PubMed: 29947147]
6. de Graav GN et al. Follicular T helper cells and humoral reactivity in kidney transplant patients. Clin. Exp. Immunol 180, 329–340 (2015). [PubMed: 25557528]
7. Bamoulid J et al. Antithymocyte globulins in renal transplantation—from lymphocyte depletion to lymphocyte activation: The doubled-edged sword. Transplant. Rev 31, 180–187 (2017).
8. Mohty M et al. New directions for rabbit antithymocyte globulin (thymoglobulin ®) in solid organ transplants, stem cell transplants and autoimmunity. Drugs 74, 1605–1634 (2014). [PubMed: 25164240]

9. Haudebourg T, Poirier N & Vanhove B Depleting T-cell subpopulations in organ transplantation. Transpl. Int 22, 509–518 (2009). [PubMed: 18980625]
10. Genestier L et al. Induction of fas (Apo-1, CD95)-mediated apoptosis of activated lymphocytes by polyclonal antithymocyte globulins. Blood 91, 2360–2368 (1998). [PubMed: 9516135]
11. Lopez M, Clarkson MR, Albin M, Sayegh MH & Najafian N A novel mechanism of action for anti-thymocyte globulin: Induction of CD4+CD25+Foxp3+ regulatory T cells. J. Am. Soc. Nephrol 17, 2844–2853 (2006). [PubMed: 16914538]
12. Grafals M et al. Immunophenotyping and efficacy of low dose ATG in non-sensitized kidney recipients undergoing early steroid withdrawal: A randomized pilot study. PLoS One 9, (2014).
13. Ayasoufi K, Fan R, Fairchild RL & Valujskikh A CD4 T Cell Help via B Cells Is Required for Lymphopenia-Induced CD8 T Cell Proliferation. J. Immunol 196, 3180–3190 (2016). [PubMed: 26912319]
14. Lei Y et al. Cathepsin S and Protease-Activated Receptor-2 Drive Alloimmunity and Immune Regulation in Kidney Allograft Rejection. Front. Cell Dev. Biol 8, 1–12 (2020). [PubMed: 32117956]
15. Mohammed MT et al. Follicular T cells mediate donor-specific antibody and rejection after solid organ transplantation. Am. J. Transplant 21, 1893–1901 (2021). [PubMed: 33421294]
16. Chen J, Chen JK, Conway EM & Harris RC Survivin mediates renal proximal tubule recovery from AKI. J. Am. Soc. Nephrol 24, 2023–2033 (2013). [PubMed: 23949800]
17. Clement RL et al. Follicular regulatory T cells control humoral and allergic immunity by restraining early B cell responses. Nat. Immunol 20, 1360–1371 (2019). [PubMed: 31477921]
18. Hart A et al. OPTN/SRTR 2019 Annual Data Report: Kidney. Am. J. Transplant 21, 21–137 (2021).
19. Kieper WC & Jameson SC Homeostatic expansion and phenotypic conversion of naïve T cells in response to self peptide/MHC ligands. Proc. Natl. Acad. Sci. U. S. A 96, 13306–13311 (1999).
20. Neujahr DC et al. Accelerated Memory Cell Homeostasis during T Cell Depletion and Approaches to Overcome It. J. Immunol 176, 4632–4639 (2006). [PubMed: 16585554]
21. Pearl JP et al. Immunocompetent T-cells with a memory-like phenotype are the dominant cell type following antibody-mediated T-cell depletion. Am. J. Transplant 5, 465–474 (2005). [PubMed: 15707400]
22. Knechtle SJ et al. Campath-1H induction plus rapamycin monotherapy for renal transplantation: Results of a pilot study. Am. J. Transplant 3, 722–730 (2003). [PubMed: 12780564]
23. Flechner SM et al. Alemtuzumab induction and sirolimus plus mycophenolate mofetil maintenance for CNI and steroid-free kidney transplant immunosuppression. Am. J. Transplant 5, 3009–3014 (2005). [PubMed: 16303017]
24. Noël C et al. Daclizumab versus antithymocyte globulin in high-immunological-risk renal transplant recipients. J. Am. Soc. Nephrol 20, 1385–1392 (2009). [PubMed: 19470677]
25. Bamoulid J et al. Anti-thymocyte globulins in kidney transplantation: Focus on current indications and long-term immunological side effects. Nephrol. Dial. Transplant 32, 1601–1608 (2017). [PubMed: 27798202]
26. Hricik DE et al. Adverse outcomes of tacrolimus withdrawal in immune-quiescent kidney transplant recipients. J. Am. Soc. Nephrol 26, 3114–3122 (2015). [PubMed: 25925687]
27. Mohammed MT & Sage PT Follicular T-cell regulation of alloantibody formation. Curr. Opin. Organ Transplant 25, 22–26 (2020). [PubMed: 31789953]
28. Macedo C et al. Impact of Induction Therapy on Circulating T Follicular Helper Cells and Subsequent Donor-Specific Antibody Formation After Kidney Transplant. Kidney Int. Reports 4, 455–469 (2019).
29. Zhang R Donor-specific antibodies in kidney transplant recipients. Clin. J. Am. Soc. Nephrol 13, 182–192 (2018). [PubMed: 28446536]
30. Wiebe C & Nickerson P Posttransplant monitoring of de novo human leukocyte antigen donor-specific antibodies in kidney transplantation. Curr. Opin. Organ Transplant 18, 470–477 (2013). [PubMed: 23695596]

31. Hatzi K et al. BCL6 orchestrates Tfh cell differentiation via multiple distinct mechanisms. J. Exp. Med 212, 539–53 (2015). [PubMed: 25824819]
32. Eto D et al. IL-21 and IL-6 are critical for different aspects of B cell immunity and redundantly induce optimal follicular helper CD4 T cell (Tfh) differentiation. PLoS One 6, e17739 (2011).
33. Poholek AC et al. In vivo regulation of Bcl6 and T follicular helper cell development. J. Immunol 185, 313–26 (2010). [PubMed: 20519643]
34. Jones JL et al. IL-21 drives secondary autoimmunity in patients with multiple sclerosis, following therapeutic lymphocyte depletion with alemtuzumab (Campath-1H). J. Clin. Invest 119, 2052–2061 (2009). [PubMed: 19546505]
35. Papillion A et al. Inhibition of IL-2 responsiveness by IL-6 is required for the generation of GC-TFH cells. Sci. Immunol 4, (2019).
36. Jogdand GM, Mohanty S & Devadas S Regulators of Tfh cell differentiation. Front. Immunol 7, 1–14 (2016). [PubMed: 26834743]
37. Crotty S Follicular helper CD4 T cells (TFH). Annu. Rev. Immunol 29, 621–63 (2011). [PubMed: 21314428]
38. Ballesteros-Tato A et al. Interleukin-2 Inhibits Germinal Center Formation by Limiting T Follicular Helper Cell Differentiation. Immunity 36, 847–856 (2012). [PubMed: 22464171]
39. Ross SH & Cantrell DA Signaling and Function of Interleukin-2 in T Lymphocytes. Annu. Rev. Immunol 36, 411–433 (2018). [PubMed: 29677473]
40. Hirai T et al. Selective expansion of regulatory T cells using an orthogonal IL-2/IL-2 receptor system facilitates transplantation tolerance. J. Clin. Invest 131, (2021).
41. Liu R et al. Expansion of regulatory T cells via IL-2/anti-IL-2 mAb complexes suppresses experimental myasthenia. Eur. J. Immunol 40, 1577–1589 (2010). [PubMed: 20352624]
42. Chung DT et al. Anti-thymocyte globulin (ATG) prevents autoimmune encephalomyelitis by expanding myelin antigen-specific Foxp3+ regulatory T cells. Int. Immunol 19, 1003–1010 (2007). [PubMed: 17698561]
43. Brennan DC, Daller JA, Lake KD, Cibrik D & Del Castillo D Rabbit Antithymocyte Globulin versus Basiliximab in Renal Transplantation. N. Engl. J. Med 355, 1967–1977 (2006). [PubMed: 17093248]

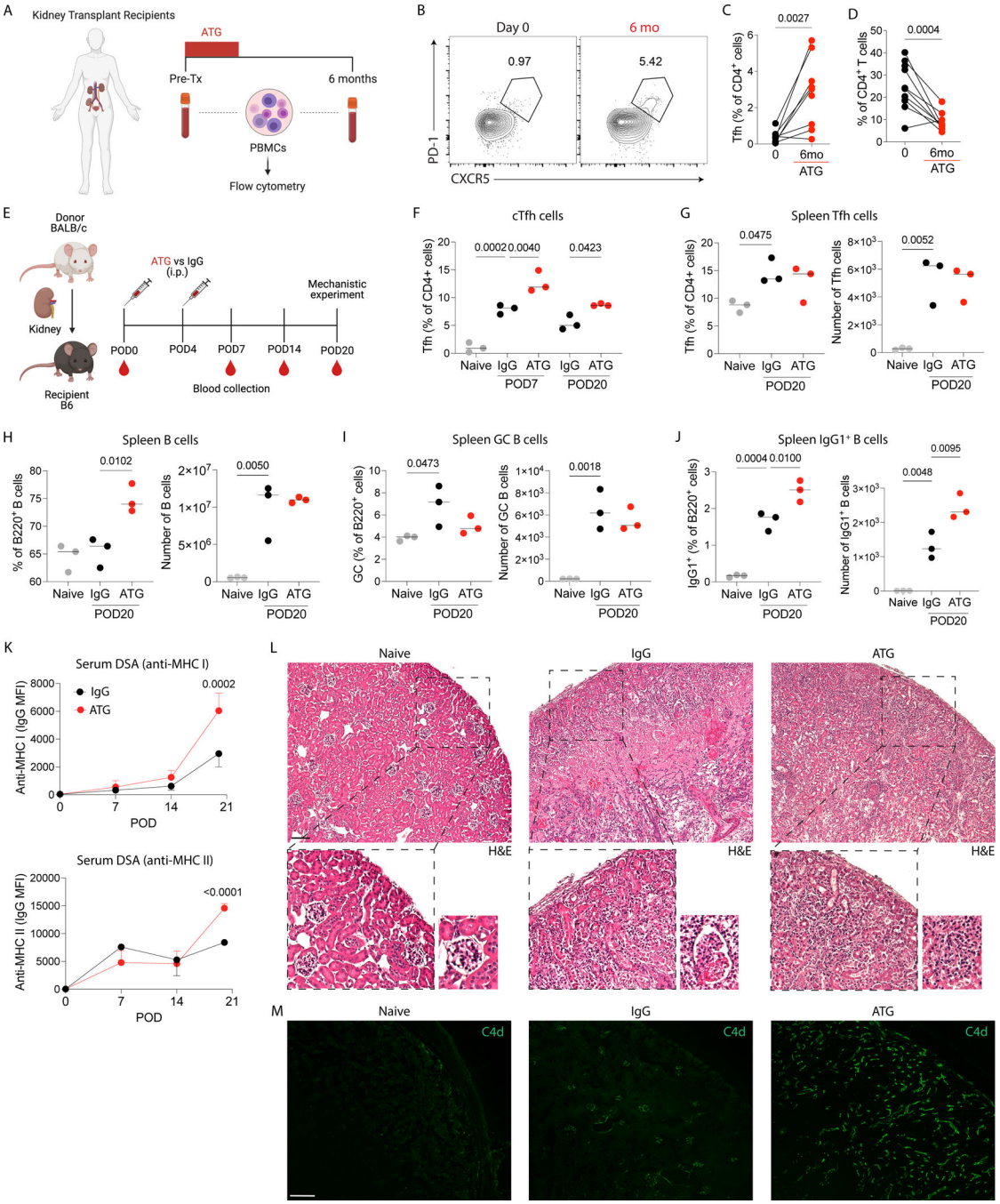

Figure 1.

ATG treatment increases the proportion of Tfh cells in kidney transplant recipients and the alloantibody response in a mouse kidney transplant model. (A) PBMCs from kidney transplant recipients before and six months after kidney transplantation were isolated and characterized by flow cytometry. (B) Representative flow cytometry contour plots, and (C) the frequency of circulating Tfh (CD4+CXCR5+PD-1+) cells and (D) total CD4+ T cells (data from 10 patients; Wilcoxon matched-pairs signed-rank test). (E) BALB/c donor kidneys were transplanted into C57Bl/6 recipients, and the recipients were intraperitoneally

treated with 500 μg of murine ATG or IgG control at POD0 and POD4. Mice were euthanized at POD20 after immunization, and blood, graft and spleens were analyzed. Naïve mice were used as additional controls. (F) The frequency of circulating Tfh cells at POD7 and POD20. The frequency and absolute cell number of (G) Tfh cells, (H) total B cells, (I) GC B cells and (J) IgG1+ B cells at POD20 in the spleen. (K) Anti-MHC I and anti-MHC II DSA quantification in the serum over time post-transplantation. (L) Representative H&E and (M) C4d staining in the grafts at POD20. Scale bar, 100 μm. (E-M) Data as mean ± SD are shown (n = 3 per group; statistic by One-Way ANOVA with Tukey multiple comparisons test).

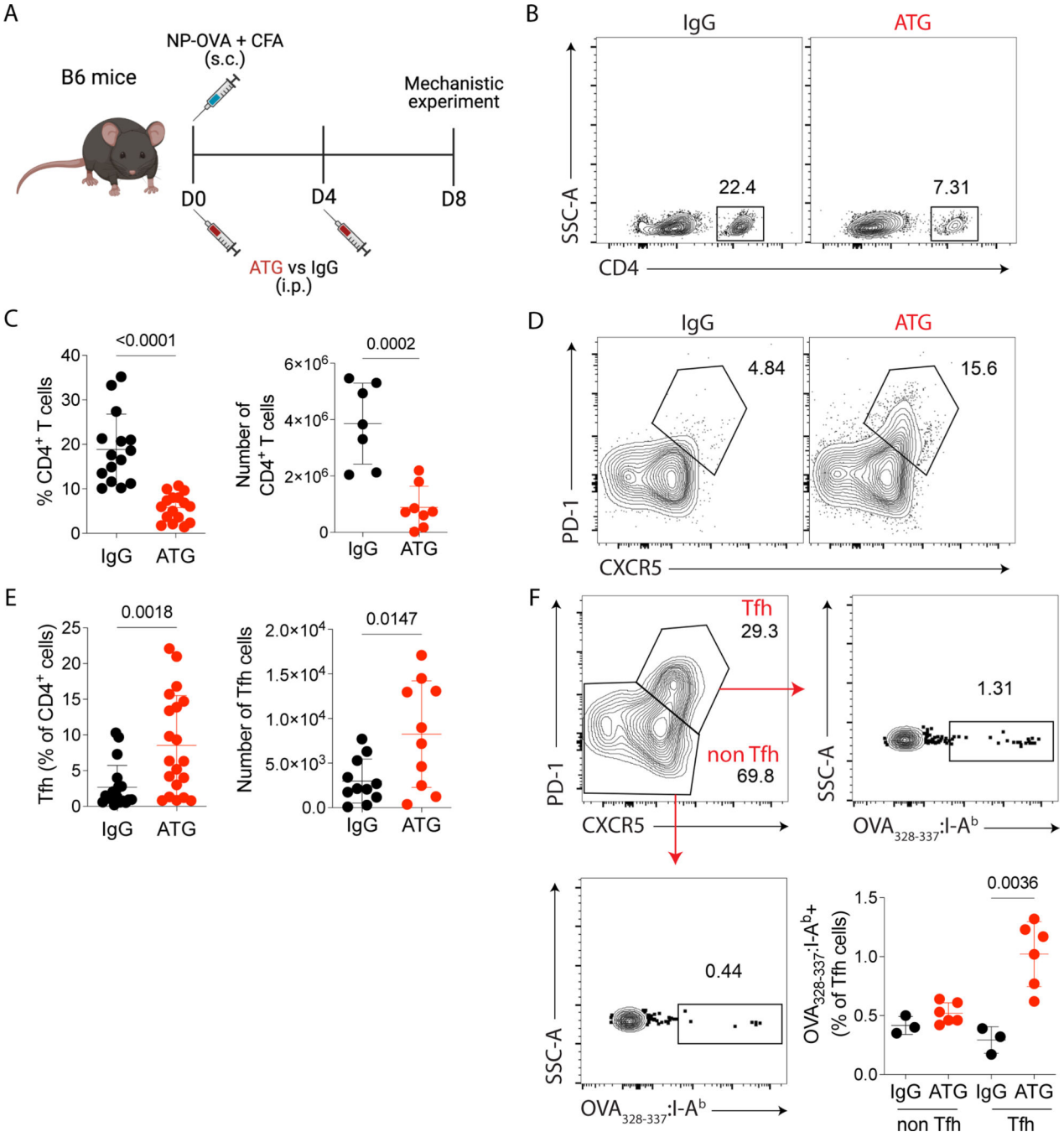

Figure 2.

ATG treatment induces antigen-specific Tfh cells expansion. (A) C57Bl/6 mice were subcutaneously immunized with NP-OVA + CFA and intraperitoneally treated with 500 μg of murine ATG or IgG control on days 0 and 4. On day 8 after immunization, lymph nodes were analyzed by flow cytometry. (B) Representative flow cytometry contour plots of CD4+ T cells in lymph nodes gated in Dump- live cells. (C) The frequency and absolute cell numbers per lymph node of total CD4+ T cells. (D) Representative flow cytometry contour plots of Tfh (CD4+CXCR5+PD-1+) cells in lymph nodes. (E) The frequency and absolute

cell number per lymph node of Tfh (CD4+CXCR5+PD-1+) cells. (F) Representative contour plots of and frequency of OVA323–339-tetramer+ cells in Tfh (CD4+CXCR5+PD-1+) and non-Tfh (CD4+CXCR5- PD-1-) cells. (A-F) Red dots represent the ATG-treated mice, and the black dots represent the IgG-treated mice. Data as mean ± SD are shown (pooled data from three independent experiments, with n = 5 per group; t-test). (C and E) Statistic by t-test. (F) Statistic by Two-way ANOVA with Tukey multiple comparisons test.

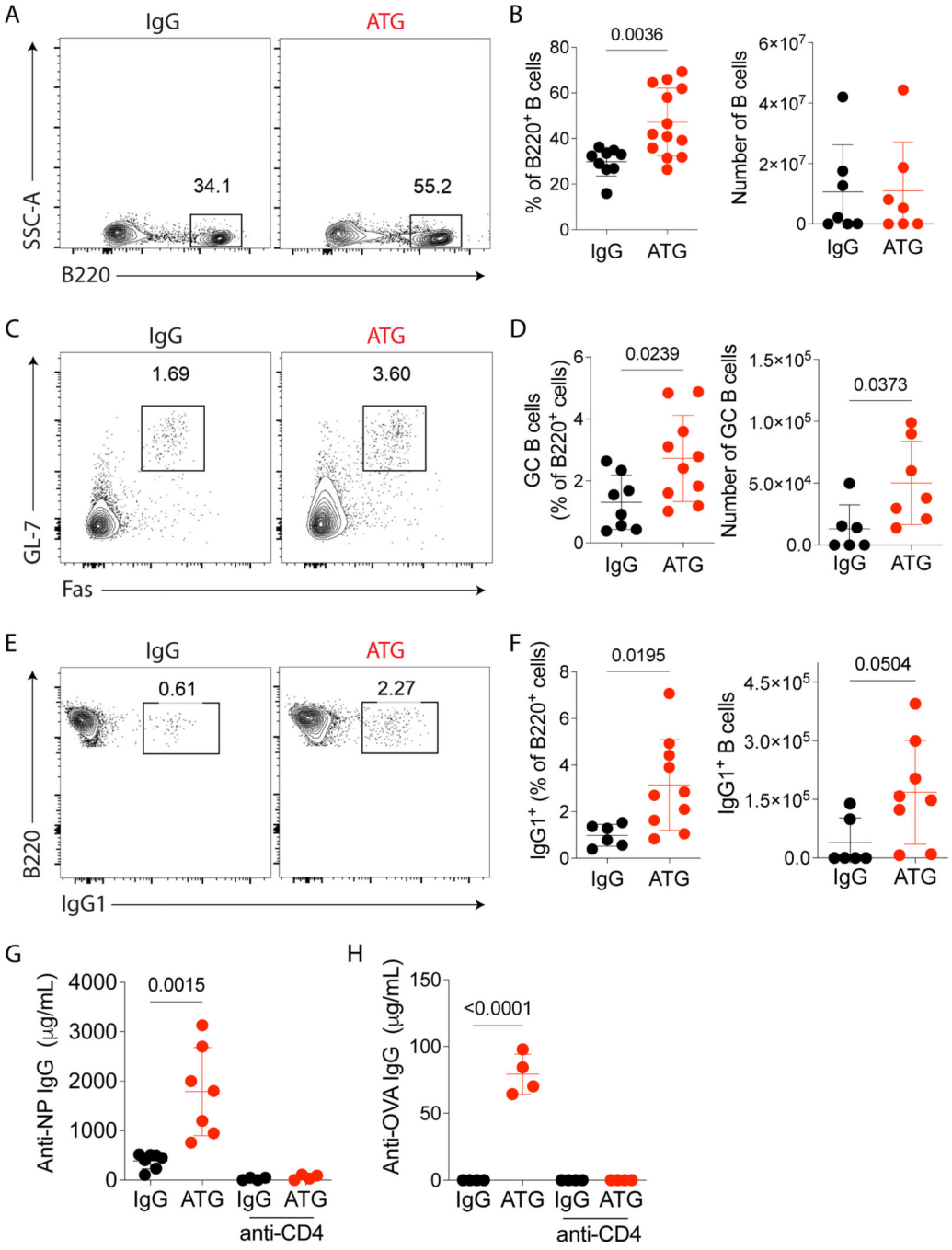

Figure 3.

ATG treatment enhances antibody-specific immune response. C57Bl/6 mice were subcutaneously immunized with NP-OVA + CFA and intraperitoneally treated with 500 μg of murine ATG or IgG control. Mice were euthanized on day 8 after immunization, lymph nodes were analyzed by flow cytometry, as shown in Fig 2A. (A) Representative contour plots of B220+ B cells in lymph nodes gated in Dump-Live cells. (B) The frequency and absolute cell number of B220+ B cells in lymph nodes. (C) Representative contour plots of GC B (B220+GL-7+Fas+) cells in lymph nodes gated in B220+ cells. (D) The

frequency and absolute cell number per lymph node of GC B cells. (E) Representative contour plots of B220+ IgG1+ cells in lymph nodes gated in B220+ cells. (F) The frequency and absolute cell number per lymph node of IgG1+ B cells. (G) ELISA quantification of serum NP-specific IgG antibodies and (H) OVA-specific IgG antibodies at day 8 after immunization in controls or ATG-treated mice with subsequent selective depletion of CD4 cells (anti-CD4 depleting antibody). (A-H) Red dots represent the ATG-treated mice, and the black dots represent the IgG-treated mice. Data as mean ± SD are shown (pooled data from three independent experiments, with n = 4–5 per group;). (B, D, and F) Statistic by t-test. (G-H) Statistic by Two-way ANOVA with Tukey multiple comparisons test.

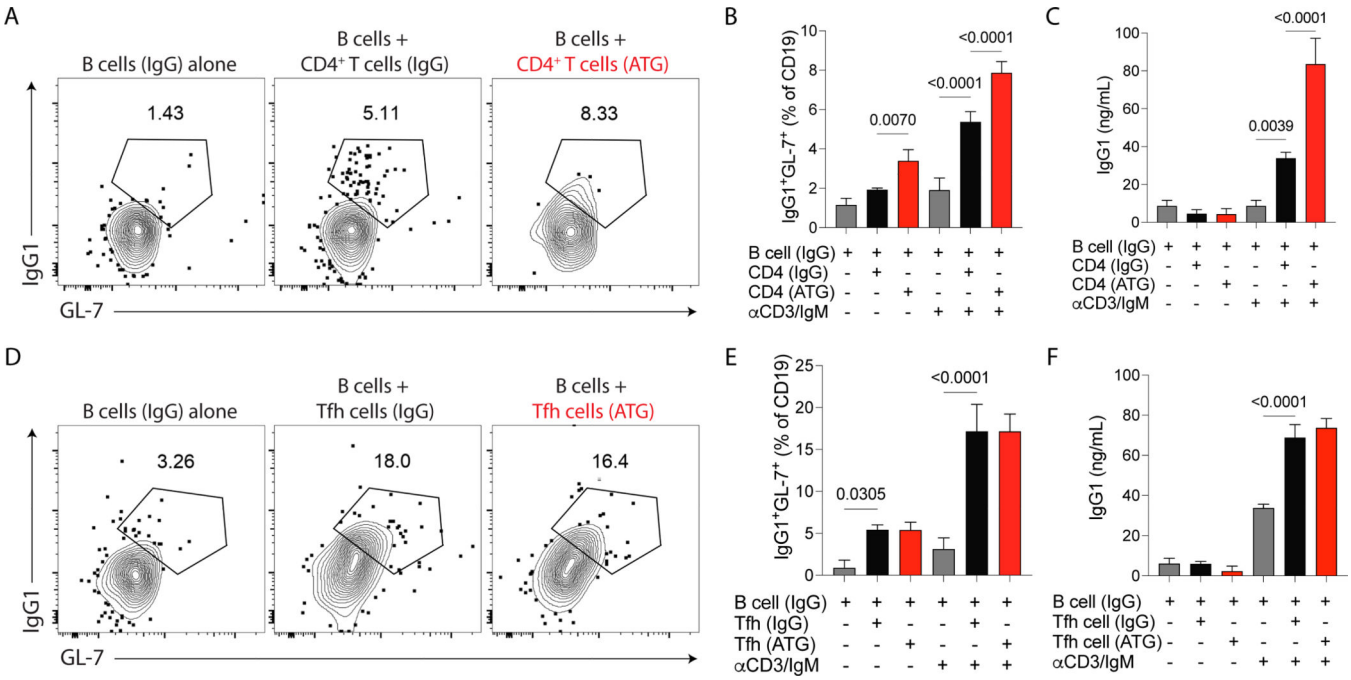

Figure 4.

Total CD4+ T cells from ATG-treated mice have an increased capacity to induce help to B cells in vitro. C57Bl/6 mice were subcutaneously immunized with NP-OVA + CFA and treated with 500 μg of murine ATG or IgG control. Mice were sacrificed at day 8 after immunization, and B cells, total CD4+ T cells or Tfh cells were sorted from the spleen and cocultured in vitro for 6 days in the presence or not of anti-CD3 and anti-IgM stimulation. (A) Representative contour plots and (B) frequency of IgG1+ GC B cells (B220+GL-7+IgG1+) in B cells cultured with total CD4+ T cells. The IgG1+ GC B cells are gated on CD19+ MHCII+ cells. (C) ELISA quantification of IgG1 antibodies in the supernatant of total CD4+ T cells cultured with B cells. (D) Representative contour plots and (E) frequency of IgG1+ GC B cells (B220+GL-7+IgG1+) in B cells cultured with total Tfh cells. The IgG1+ GC B cells are gated on CD19+ MHCII+ cells. (F) ELISA quantification of IgG1 antibodies in the supernatant of Tfh cells cultured with B cells. (A-F) All the B cells were from IgG-treated animals. Grey bars represent B cells alone, the black bars represent B cells coculture with CD4+ T cells or Tfh cells from IgG-treated mice, and the red bars represent B cells coculture with CD4+ T cells or Tfh cells from ATG-treated mice. Data as mean ± SD are shown (pooled data from three independent experiments; One-way ANOVA with Tukey multiple comparisons test).

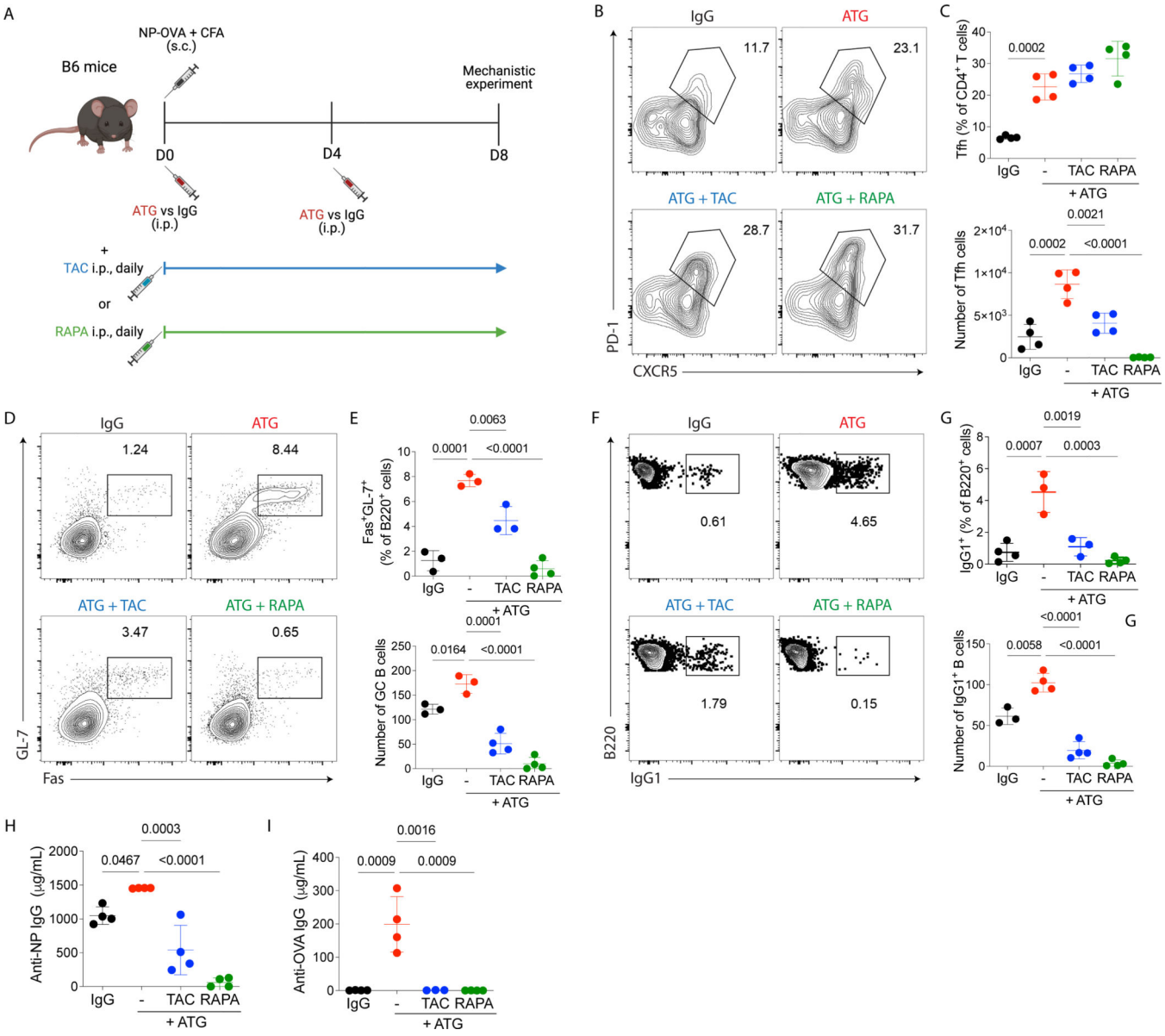

Figure 5.

ATG combinations with tacrolimus or rapamycin control humoral response induced by ATG treatment alone. (A) C57Bl/6 mice were subcutaneously immunized with NP-OVA + CFA and treated with 500μg of murine ATG or IgG control. A subgroup then received either 1 mg/Kg of tacrolimus or 0.5 mg/Kg of rapamycin, intraperitoneally, daily. Mice were euthanized at day 8 after immunization, and serum and lymph nodes were analyzed, as shown in Fig 2A. (B) Representative contour plots of Tfh (CD4+CXCR5+ PD-1+) cells in lymph nodes gated in CD4+ cells. (C) The frequency and absolute cell number per lymph node of Tfh cells. (D) Representative contour plots of GC B (B220+GL-7+ Fas+) cells in lymph nodes gated in B220+ cells. (E) The frequency and absolute cell number per lymph node of GC B cells. (F) Representative contour plots of B220+ IgG1+ cells in lymph nodes gated in B220+ cells. (G) The frequency and absolute cell number per lymph node of IgG1+

B cells. ELISA quantification of serum (H) NP-specific and (I) OVA-Specific IgG antibodies at day 8 after immunization. (A-I) Red dots represent the ATG-treated mice, black dots represent the IgG-treated mice, blue dots represent the ATG + tacrolimus-treated mice, and green dots represent the ATG + rapamycin-treated mice. Data as mean ± SD are shown (data from three independent experiments; with n = 4 per group; One-way ANOVA with Tukey multiple comparisons test).

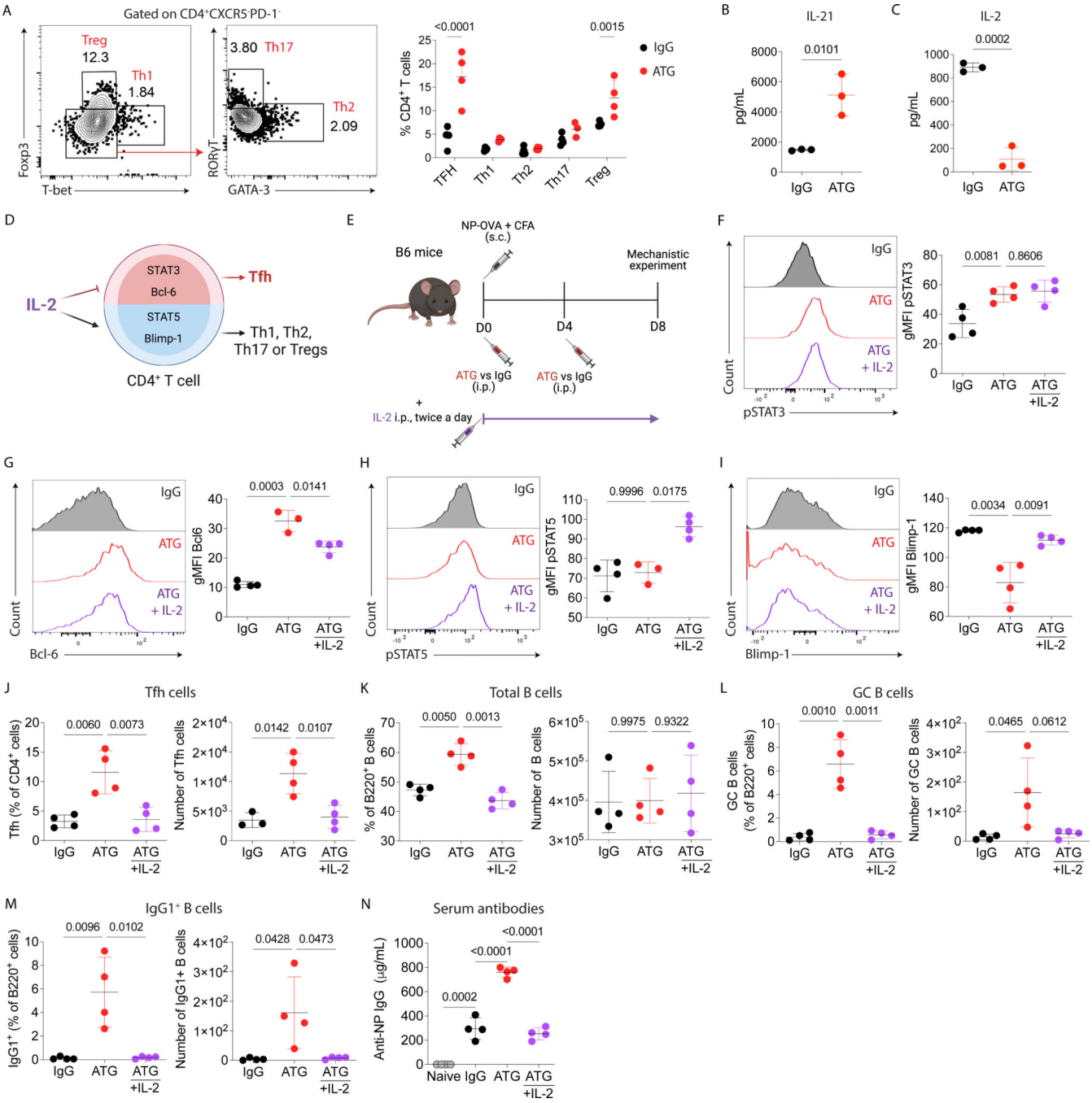

Figure 6.

IL-2 signaling inhibits ATG-mediated humoral response. Using the NP-OVA + CFA immunization with either IgG or ATG treatment as shown in Fig 1D, we determined (A) the frequency of Tfh (CD4+CXCR5+PD-1+), Th1 (CD4+CXCR5-PD-1-FOXP3-Tbet+), Th2 (CD4+CXCR5-PD-1-FOXP3-Tbet-Gata3+), Th17 (CD4+CXCR5-PD-1-FOXP3-Tbet-RORγT+), and Treg (CD4+CXCR5- PD-1-FOXP3+ Tbet-) cells at day 8 after NP-OVA + CFA immunization in lymph nodes, (B) serum IL-21 levels after 48 hours of immunization with NP-OVA+CFA, and the (C) serum IL-2 levels after 6 hours of immunization with

NP-OVA + CFA with IgG or ATG treatment. (D) Cartoon of the IL-2 signaling pathway in CD4+ T cell differentiation. (E) C57Bl/6 mice were subcutaneously immunized with NP-OVA+CFA and treated with 500 μg of murine ATG or IgG control. A subgroup then received ATG and 30,000 U of recombinant mouse IL-2, intraperitoneally, twice a day. Mice were euthanized at day 8 after immunization, and serum and lymph nodes were analyzed, as shown in Fig 2A. Quantification of the geometric mean fluorescence intensity (gMFI) of (F) pSTAT3, (G) Bcl6, (H) pSTAT5, and (I) Blimp-1 in CD4+ T cells from draining lymph nodes. Red histograms and red dots represent the ATG-treated mice, black histogram and dots represent the IgG-treated mice, and the purple histograms and dots represent the ATG-treated mice that received IL-2. The frequency and absolute cell number of (J) Tfh cells, (K) total B cells, (L) GC B cells, and (M) IgG1+ B cells in the draining lymph node. (N) ELISA quantification of serum NP-specific IgG antibodies at day 8 after immunization. Naïve mice were used as additional controls. Data as mean ± SD are shown (n = 4 per group; One-way ANOVA with Tukey multiple comparisons test).